Acta Oncologica, 2014; 53: 1019–1026

informa
healthcare

ORIGINAL ARTICLE

Isocentric integration of intensity-modulated radiotherapy with electron fields improves field junction dose uniformity in postmastectomy radiotherapy

PAULIINA WRIGHT[1,2], SAMI SUILAMO[1,2], PAULA LINDHOLM[2] & JARMO KULMALA[1,2]

[1]*Department of Medical Physics, Turku University Hospital, Finland and* [2]*Department of Oncology, Turku University Hospital, Finland*

ABSTRACT

Background. In postmastectomy radiotherapy (PMRT), the dose coverage of the planning target volume (PTV) with additional margins, including the chest wall, supraclavicular, interpectoral, internal mammary and axillar level I–III lymph nodes, is often compromised. Electron fields may improve the medial dose coverage while maintaining organ at risk (OAR) doses at an acceptable level, but at the cost of hot and cold spots at the electron and photon field junction. To improve PMRT dose coverage and uniformity, an isocentric technique combining tangential intensity-modulated (IM)RT fields with one medial electron field was implemented.

Material and methods. For 10 postmastectomy patients isocentric IMRT with electron plans were created and compared with a standard electron/photon mix and a standard tangent technique. PTV dose uniformity was evaluated based on the tolerance range (TR), i.e. the ratio of the standard deviation to the mean dose, a dice similarity coefficient (DSC) and the 90% isodose coverage and the hot spot volumes. OAR and contralateral breast doses were also recorded.

Results. IMRT with electrons significantly improved the PTV dose homogeneity and conformity based on the TR and DSC values when compared with the standard electron/photon and tangent technique ($p < 0.02$). The 90% isodose coverage improved to 86% compared with 82% and 80% for the standard techniques ($p < 0.02$). Compared with the standard electron/photon mix, IMRT smoothed the dose gradient in the electron and photon field junction and the volumes receiving a dose of 110% or more were reduced by a third. For all three strategies, the OAR and contralateral breast doses were within clinically tolerable limits.

Conclusion. Based on these results two-field IMRT combined with an electron field is a suitable strategy for PMRT.

Postmastectomy radiotherapy (PMRT) in node-positive breast cancer is widely used and has proven to reduce the locoregional and overall recurrence as well as breast cancer mortality [1]. However, the dose coverage of the whole planning target volume (PTV), comprising the chest wall, supraclavicular, interpectoral, internal mammary and axillar level I–III lymph nodes and additional margins, is often compromised. A common technique for radiotherapy delivery is to use opposing tangential photon fields for the chest wall and anterior/posterior fields for the superior PTV [2,3]. However, organs at risk (OARs) and the contralateral breast dose limit the achievable dose coverage both medially and to the axillary lymph nodes. Although these obstacles have partly been overcome by mixing electron and photon beams [3,4], issues regarding the field junction hot and cold spots remain.

Intensity-modulated radiotherapy (IMRT) has the potential of tailoring the dose better to the chest wall, but requires between seven or 11 fields and the contralateral breast low dose volume is significantly increased [5–8]. Clinical implementation is therefore limited by the minor, but significant, increased risk of secondary cancer proven for radiotherapy associated sites [9,10]. Multibeam IMRT incorporated with electron fields reduces the contralateral breast doses, but still results in significantly higher doses than conformal RT [5]. Furthermore, field-in-field

Correspondence: P. Wright, Turku University Hospital, Department of Radiotherapy (T-hospital), PO Box 52, 20521 Turku, Finland. Tel: +35 823131808. E-mail: pauliina.wright@tyks.fi

(Received 16 April 2014; accepted 14 May 2014)

ISSN 0284-186X print/ISSN 1651-226X online © 2014 Informa Healthcare
DOI: 10.3109/0284186X.2014.926027

photon fields in combination with electrons may improve the field junction dose uniformity [11,12], but compared with dynamic IMRT the drawback is a less conformal dose distribution.

The aim of this study was to investigate if isocentrically delivered two-field dynamic IMRT with a medial electron field could be used to improve the field junction dose uniformity. Two-field IMRT would not be expected to remarkably increase the contralateral breast dose when compared with a conformal treatment or multibeam IMRT. Comparison was made with the standard electron/photon mix used in PMRT at Turku University Hospital (TUH) department and with a standard tangential technique.

Material and methods

Patient material

Since the intent was to deliver photon and electron beams isocentrically, the risk for gantry and couch collision limited the chest wall height in the treatment position to a maximum of 28 cm. Ten female breast cancer patients referred for PMRT, five left- and five right-sided, were included in this planning study. Their average body mass index was 24.2 (range 21.2–29.1 kg/m^2) and age was 58 years (range 34–92 years). For CT acquisition the patients were placed in the supine treatment position and immobilized using a breastboard with both arms raised above their heads (Posirest–2, CIVCO Medical Systems, Kalona, IW, USA). All images were acquired in free breathing with a slice thickness of 2.5 mm (GE LightSpeed RT 16; General Electric Medical Systems, Milwaukee, WI, USA). Contouring of the PTV and OARs as well as treatment plan calculations were made in the Eclipse treatment planning system (Eclipse 10.0 and 11.0, Varian medical Systems, Palo Alto, CA, USA). The PTV comprised the chest wall from skin surface to the pleural cavity and included the pectoral muscles, the supraclavicular, interpectoral, internal mammary level I–III and axillar level I–III lymph nodes with setup margins. Inferiorly the PTV reached approximately 1 cm below the contralateral breast and medially to the sternum's mid-line. Contoured OARs were both lungs, the spinal cord, the heart, the brachial plexus, the thyroid, the glenohumeral joint and the contralateral breast. An overview of the investigated treatment strategies and the PTV outline is displayed in Figure 1.

Treatment planning

According to general guidelines [2,13] the prescribed dose was set to 50 Gy in 25 fractions. Three treatment plans were generated for each patient: 1) isocentric IMRT and a medial electron field (IMRT with electrons); 2) the standard electron/photon mix and; 3) standard tangents, as described below.

The isocentric IMRT with electron treatment plans combined two wide tangential IMRT fields with a medial electron field. To manage isocentric treatment with the electron applicator the anterior source to skin distance (SSD) was set 102–104 cm. The gantry angle of the electron field was 8°–18° to the contralateral side, according to patient anatomy. A Lipowitz' alloy block was used to individually shape the electron field to treat the thinnest part of the chest wall adjacent to the lung. Based on the PTV thickness the electron beam energy was set to either 6 MeV or 9 MeV for the patients in question. Final adjustment of the 95% isodose to reach the posterior PTV border was made by manually setting the monitor units (MUs). When applicable, bolus of thickness 3 mm, 6 mm or 9 mm was used to conform the electron field dose. After dose calculation the electron field dose distribution was used as a base plan in the Eclipse IMRT dose volume optimizer (DVO 10.0.28 or 11.0.31). The anterior IMRT field (energy 6 MV) was set to 15°–25° and the posterior (energy 6 MV or 10 MV) approximately opposing it (180° ± 18°). Collimator rotation for the IMRT fields was selected such that the maximum field width was 13.9 cm, thus avoiding split fields during optimization and multiple leaf collimator (MLC, Varian 120 Millenium Leaf) motion calculation. PTV dose optimization objectives were set to 100% of the volume to receive a minimum of 49.5 Gy and 0% a maximum of 50.5 Gy. To further reduce hot spots, constraints on upper doses of 52.5 Gy and 55 Gy were used. The ipsilateral lung dose was limited by introducing patient-specific optimization objectives. To avoid hot spots outside the PTV, optimization constraints were also set for the volume of normal tissue. After optimization, the fluences were manually smoothed to reduce beam modulation and to allow for a 1.5 cm skin flash to account for setup and respiratory variability of the body outline. Smoothing was carried out with a 2.5 cm wide pencil all over the field fluences.

The standard, non-isocentric, electron/photon mix used combines two opposing anterior–posterior electron fields with an anterior electron beam. The anterior photon and electron fields are directly matched on the skin surface by setting the MLCs according to the electron block edge. The isocentric standard tangent plans consisted of two opposing tangential fields on the chest wall matched with AP and PA fields covering the upper part of the PTV. The common isocentric was set level with the lung apex. Beam energies used for the standard plans were 6 MV, 15 MV for photons and 6 MeV and 9 MeV for electrons. For details on the two standard techniques, see Appendix (available online at: http://informahealthcare.com/doi/abs/10.3109/0284186X.2014.926027).

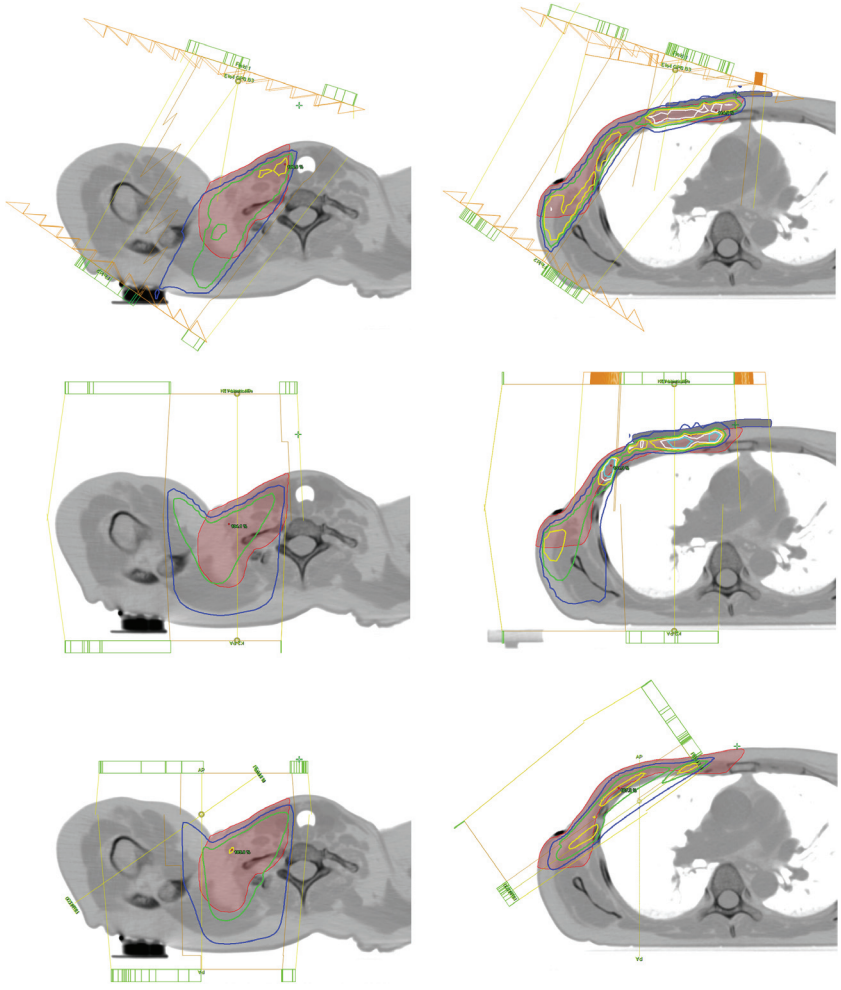

Figure 1. Overview of the three treatment techniques. Top panel: IMRT with electrons, middle: standard electron/photon mix and lower panel: standard tangents. The PTV outline (red shaded area) and field arrangements at the level of the supraclavicular fossa (left) and at mid chest wall (right). Isodoses: blue 90% (45 Gy), green 100% (50 Gy), yellow 105% (52.5 Gy), white 110% (55 Gy) and cyan 115% (57.7 Gy) of the prescribed dose.

All treatment plans were normalized to 100% median dose. Photon and electron field doses were calculated with the Anisotropic Analytic Algorithm and the Generalized Gaussian Pencil Beam (versions 11.0.31), respectively. The respective calculation grids were set to 0.2 cm and 0.5 cm. Accepted ipsilateral lung doses were $V_{20Gy} \leq 35\%$ and mean dose ≤ 18 Gy. Heart mean doses were kept as low as possible, without compromising the PTV dose coverage. Dose outside the PTV was limited to <55 Gy (110% of the prescribed dose).

Treatment plan evaluation and comparison

Evaluation of the treatment plans was based on PTV dose homogeneity and conformity, dose coverage and hot spot volumes as well as OAR doses. PTV dose homogeneity estimates was evaluated with the tolerance range (TR) [14] and conformity with the dice similarity coefficient (DSC) for the 90% isodose volume. For definitions see Appendix available online at: http://informahealthcare.com/doi/abs/10.3109/0284186X.2014.926027. All PTV characteristics were calculated for the full PTV, i.e. extending to the skin surface. Statistical significance of the PTV dose statistics was tested with the Wilcoxon signed rank two-tailed test. The OAR doses are significantly affected by PTV dose coverage. Therefore, evaluation of the investigated methods based on p-values for OAR dose characteristics could be misleading. Instead, the evaluation of the proposed method is based on the treatment plans restricted by clinically acceptable OAR doses. Further, the photon and, where applicable, electron MUs were recorded for all treatment plans.

Verification

Verification of the IMRT and electron field junction dose was carried out with EBT2 film (Gafchromic EBT2, Wayne, NJ, USA) at 1.4 cm depth in a $10 \times 30 \times 30$ cm (height $\times$ width $\times$ length) phantom of

water-equivalent polystyrene. The irradiated radiographic films were scanned at 48-bit, 72 dpi using the red channel of a flatbed scanner (Epson Perfection V7000, Seiko Epson Corporation, Nagano, Japan). To reduce the effect of scanner non-flatness a mask of irradiated Gafchromic film was applied, while calibration between analog to digital conversion (ADC) values was carried out with reference films irradiated between 0 and 3 Gy. Calculated and measured dose planes were compared using OmniPro-IMRT (version 1.6, IBA Dosimetry GmbH, Schwarzenbruck, Germany). Since calibration measurements showed that the photon versus electron film responses disagreed by 1–2%, the acceptance limit for the verification measurements was set to 5%. Finally, the stability of the IMRT and electron field junction was evaluated by simulating a setup error, i.e. a latitude offset of ± 3 mm for the electron field in the treatment planning system. The resulting changes in dose maximum and $V_{90\%}$ coverage of the PTV were recorded.

Results

IMRT with electrons significantly improved the PTV dose homogeneity and conformity in terms of the TR and DSC, respectively, as well as the 90% dose coverage when compared with the two standard techniques. Specific values for PTV dose characteristics are found in Table I. The lowest TR was found with IMRT and electrons for all patients. Furthermore, IMRT with electrons improved chest wall dose uniformity and resulted in smaller $V_{110\%}$ and $V_{120\%}$ volumes as compared with the standard electron/photon mix (p-value < 0.02). The reduction of hot spot volumes steepened the PTV dose gradient as seen from the average DVHs over all patients displayed in Figure 2. Most homogeneous chest wall dose was achieved with standard tangents with no significant continuous volumes with doses over 110%. However, the field widths had to be limited to keep the ipsilateral lung dose within acceptable limits, resulting in underdosage of the medial and deep axillary parts of the PTV.

Dose characteristics for the ipsi- and contralateral lung, spinal cord, brachial plexus, heart, glenohumeral joint, thyroid as well as the contralateral breast are found in Table II. For the ipsilateral lung the percentage volume receiving less than 20 Gy (V_{20Gy}) was reduced by standard tangents, while the mean doses were similar with all three strategies, for DVHs see Figure 3. Application of the electron field reduced the V_{30Gy} to an average of 20.4% and 21.6% with IMRT and the standard mix, respectively, compared with the average value of 27.9% for the standard tangential treatment. Correspondingly the V_{1Gy} for the contralateral breast was approximately halved by the electron field in both the IMRT and electron or standard electron/photon mix plans. For left-sided patients, mean heart doses between 2.5 and 4.1 Gy were recorded with the three strategies, while the highest dose maximum of nearly 50 Gy for a volume of at least 1 cm^3 resulted from the tangential technique. For right-sided patients the heart mean dose was similar with all strategies, while maximum doses increased with the electron techniques. The selected field arrangement for the IMRT with electron plans roughly halved the average maximum spinal cord dose to 16.3 Gy from 29.0 Gy and 37.9 Gy with the standard electron/photon mix and tangents. Correspondingly the glenohumeral joint doses were increased to 32.0 Gy from 16.6 Gy and 23.1 Gy with the standard techniques. Considering the brachial plexus, thyroid and contralateral lung maximum respectively mean doses were similar with all strategies.

On average, the photon MUs were 475 (range 370–572, SD 55) for IMRT with electrons, 260 (243–271, SD 10) with standard electron/photon mix and 454 (423–508, SD 25) with standard tangents. Correspondingly, average electron field MUs were 215 (range 192–228, SD 11) for the IMRT with electron plans and 232 (229–235, SD 4) for the standard electron/photon plans. With the standard electron/photon mix three of the patients required two

Table I. Dose characteristics of the PTV for the tangential IMRT with electron, standard electron/photon mix and standard tangents. Treatment plans were normalized to a median dose of 100% (50 Gy). All values calculated for the full PTV extending to the body surface.

	IMRT with electron		Standard electron/photon		Standard tangents	
	Mean ± SD	(range)	Mean ± SD	(range)	Mean ± SD	(range)
Mean dose (%)	97.3 ± 0.5	(96.0–98.7)	96.1 ± 0.6*	(94.3–97.9)	93.2 ± 1.6*	(86.7–97.0)
V_{45Gy} (%)	85.5 ± 3.6	(78.5–91.1)	82.3 ± 2.4*	(79.6–86.1)	80.4 ± 5.7*	(71.4–87.6)
V_{55Gy} (cm^3)	46.7 ± 31.4	(7.2–113.1)	74.9 ± 31.8*	(27.8–120.3)	0.6 ± 0.9*	(0.0–2.3)
V_{60Gy} (cm^3)	2.1 ± 2.6	(0–8.6)	8.4 ± 5.3*	(1.7–18.2)	0.0 ± 0.0*	(0–0)
TR	0.11 ± 0.03	(0.05–0.14)	0.15 ± 0.02*	(0.12–0.19)	0.20 ± 0.07*	(0.11–0.32)
DSC	0.52 ± 0.05	(0.44–0.59)	0.45 ± 0.07*	(0.37–0.54)	0.46 ± 0.05*	(0.39–0.51)

DSC, dice similarity coefficient; TR, tolerance range. *Significant difference as compared with the IMRT with electron technique (p-value ≤ 0.02).

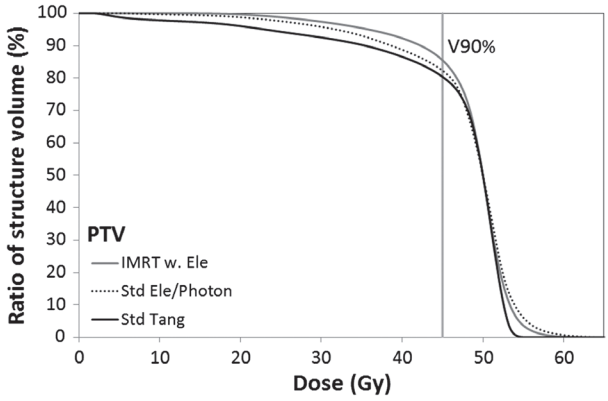

Figure 2. Averaged DVHs of the PTV dose. V_{45Gy}, i.e. 90% of the prescribed dose highlighted by the vertical line.

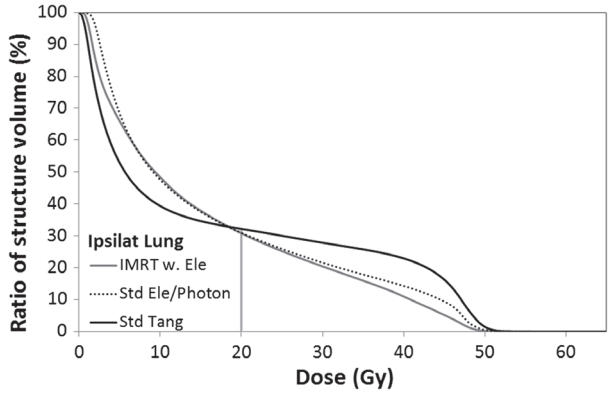

Figure 3. Averaged DVHs of the ipsilateral lung dose. V_{20Gy} highlighted by the vertical line.

electron energies for optimal dose coverage. The total electron MUs for these standard electron/photon plans were between 454 and 470. With IMRT and electrons, the tangential beam arrangement allowed the treatment of a larger part of the chest wall with photons and no split electron fields were required.

The calculated and measured IMRT with electron dose distributions showed good agreement and in the field junction $>90\%$ of the 3×3 mm pixels agreed within 5% (Figure 4). Larger deviations were observed at the film edges and at the field junction. A lateral 3 mm shift of the electron field border increased the dose maximum by 7% on average, while the 90% dose coverage of the PTV was nearly unchanged. Correspondingly a medial shift decreased both the dose maximum by 1% on average and the 90% dose coverage by 2%, details in Supplementary Table I (available online at: http://informahealthcare.com/doi/abs/10.3109/0284186X.2014.926027).

Discussion

This study presents a method that combines two-field tangential IMRT with a medial electron field in postmastectomy RT. Based on the TR and DSC values, the method presented significantly improved PTV dose uniformity and conformity when compared with the two standard techniques. IMRT reduced the electron and photon field junction hot and cold spots as seen from Table I and Figure 2. In a study by Tenhunen et al. [11] with an anterior–posterior beam arrangement, a field-in-field technique reduced the PTV hot spots when compared with a standard electron/photon mix, while the best PTV dose coverage was achieved with a conformal tangential treatment. The study [11] reported 15% of the PTV receiving more than 107% (53.5 Gy) of the prescribed dose. Based on Figure 2 this value is approximately 5% with the current method when

Table II. OAR dose characteristics.

		IMRT with electron		Standard electron/photon		Standard tangents	
		Mean ± SD	(range)	Mean ± SD	(range)	Mean ± SD	(range)
Ipsilat lung	V_{20Gy} (%)	30.6 ± 3.8	(22.6–34.6)	30.9 ± 2.6	(27.8–35.3)	32.2 ± 2.3	(29.4–35.2)
	V_{30Gy} (%)	20.4 ± 3.2	(15.1–23.5)	21.6 ± 1.9	(18.6–24.1)	27.9 ± 1.6	(26.3–31.2)
	Mean dose (Gy)	15.4 ± 1.4	(12.4–16.9)	16.3 ± 0.9	(15.0–17.6)	16.4 ± 0.7	(15.3–17.6)
C.lat lung	Mean dose (Gy)	0.4 ± 0.1	(0.4–0.7)	0.6 ± 0.2	(0.3–1.1)	0.4 ± 0.1	(0.4–0.7)
Spinal cord	Max dose (Gy)	14.3 ± 8.8	(3.3–29.6)	29.0 ± 2.2	(24.0–31.7)	35.5 ± 8.3	(21.4–45.4)
Brachial plexus	Max dose (Gy)	50.9 ± 0.9	(49.3–52.1)	50.8 ± 1.0	(49.0–52.2)	51.5 ± 1.0	(50.3–53.1)
Heart/left-sided patients	Mean dose (Gy)	2.5 ± 1.4	(1.6–4.9)	3.1 ± 1.4	(2.0–5.5)	4.1 ± 2.8	(1.6–7.7)
	Max dose (Gy)	20.4 ± 8.9	(13.7–35.9)	22.5 ± 14.3	(5.4–40.5)	43.8 ± 7.7	(30.4–49.8)
Heart/right-sided patients	Mean dose (Gy)	0.8 ± 0.3	(0.5–1.3)	1.1 ± 0.4	(0.6–1.4)	0.7 ± 0.2	(0.5–1.3)
	Max dose (Gy)	10.8 ± 6.2	(5.7–18.0)	12.0 ± 8.2	(4.1–21.6)	3.6 ± 0.3	(3.4–4.1)
C.lat breast	V_{1Gy} (cm^3)	81.1 ± 19.0	(60.7–110.3)	82.4 ± 30.8	(39.5–127.5)	150.8 ± 33.6	(85.0–192.5)
	V_{3Gy} (cm^3)	17.7 ± 8.2	(6.3–28.9)	18.2 ± 16.7	(0.0–46.7)	13.8 ± 9.5	(2.2–30.7)
	Max (Gy)	13.1 ± 7.7	(4.8–27.5)	10.1 ± 27.4	(2.1–27.4)	6.5 ± 3.9	(3.2–14.0)
Humeral joint	Mean dose (Gy)	30.3 ± 7.6	(16.6–40.5)	14.2 ± 11.6	(5.4–34.2)	21.7 ± 7.4	(8.9–35.2)
Thyroid	Mean dose (Gy)	22.3 ± 5.6	(14.6–31.5)	18.2 ± 7.1	(9.0–34.9)	19.3 ± 7.4	(4.6–28.1)

Spinal cord and brachial plexus maximum doses are defined as the point maximum, while heart and contralateral breast maximum dose is the maximum dose to a volume of at least 1 cm^3. C. lat, contralateral.

considering the 10 patients investigated. The method presented here has both the benefit of a smoother field junction dose from IMRT and improved dose coverage with a tangential field setup. Within acceptable hot spot limits it would further be possible to increase the internal mammary lymph node dose coverage with the suggested method. However, manual smoothing was required since it was not possible to achieve a favorable fluence distribution solely by optimization.

The electron field dose distributions in this study were calculated with the generalized Gaussian pencil beam algorithm, which may cause inaccuracies due to tissue heterogeneities. Oblique electron beam angles are expected to increase the impact of these inaccuracies. To reduce this effect, the maximum electron beam angle was limited to 18° in the current study. Furthermore, increased beam modulation could be expected to enhance the inaccuracies, especially in the field junction. Smoothing of the IMRT fluences with a wide pencil is therefore crucial. However the electron energies used were 6 MeV and 9 MeV, both with a little contribution of secondary photons. With increasing energies, pencil beam based algorithms may, e.g. underestimate lung dose, while Monte Carlo-based algorithms tend to underestimate dose deposited to air at lower beam energies [15]. Before clinical implementation, at least with higher beam energies, verification measurements should be carried out to investigate which calculation algorithm is preferable for each energy. For verification purposes, calculated dose distribution could also be compared to Monte Carlo simulations [15].

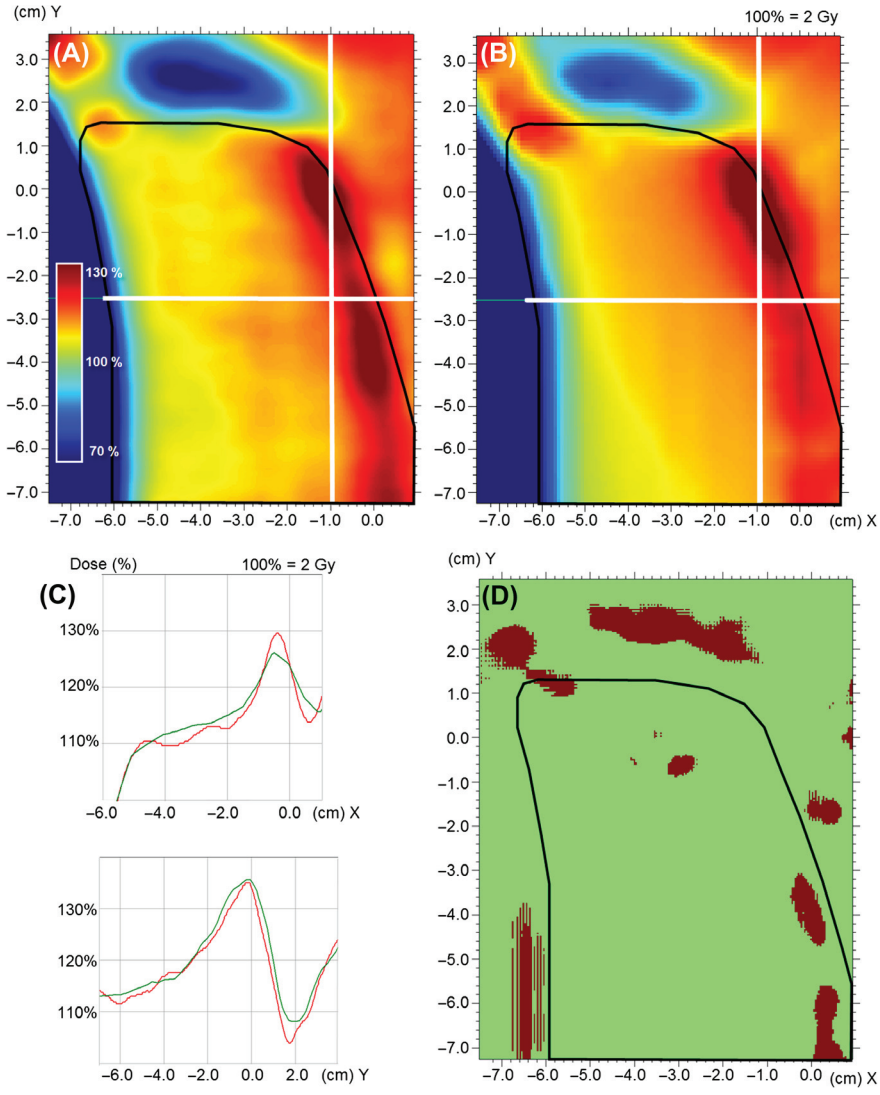

Figure 4. Measured (A) and calculated (B) frontal dose distributions for the field junction of an IMRT with electron treatment plan. The electron block border indicated by the black line. Line profiles (C) in the directions of the horizontal and vertical white lines, red and green profiles represent the measured and calculated doses, respectively. Gamma plot (D) calculated for 5% deviation within 3 mm, discrepancies > 5% displayed in red.

The achieved improvement in the electron and photon field junction dose uniformity was verified by film measurements in the homogeneous polystyrene phantom (Figure 4). The observed deviations $>5\%$ in the field junction could result from setup variation of the electron block. Combining electron and photon fields is dosimetrically challenging as it is not certain that the electron field is exactly centered throughout all treatment fractions. Despite the 3 mm displacement introduced to the electron field border, the 90% dose coverage was nearly maintained and the resulting hot spots were within the limits achieved with a perfect setup using the standard electron/photon technique (see Supplementary Table I available online at: http://informahealthcare.com/doi/abs/10.3109/0284186X.2014.926027). Furthermore, a 3 mm shift represents a rather large mismatch error, and it is therefore realistic to assume that the simulation represents the worst case scenario.

OAR doses with all the investigated methods were within clinically acceptable limits. Both the V_{20Gy} and mean lung dose have been reported as predictors for radiation-induced pneumonitis, while lung fibrosis appears to be related to V_{30Gy} [16,17]. Therefore, the presented results indicate that the risk for radiation-induced pneumonitis is similar between the techniques, while the use of an electron field reduces the risk for lung fibrosis.

There is an excess risk of secondary malignancies among long-term survivors of breast cancer [9,10]. Multifield IMRT as well as volumetric modified arc therapies increase the low dose volume, which may increase the risk for radiation-induced cancers. Since photon fields result in more scatter than electron fields, the photon MUs are more crucial for the resulting low dose volumes. For IMRT and electrons, the rather large variation of 370–572 MUs for photon fields was mostly due to patient anatomy. Although IMRT increased the photon MUs as compared with the standard electron/photon technique, they were still comparable with those produced by the standard field-in-field tangent technique. Despite the improved dose coverage resulting from IMRT with electrons, the contralateral breast V_{1Gy} compared to standard tangents was reduced by approximately half. However, the improved medial dose coverage achieved with the electron field increased the V_{3Gy} and the maximum dose. A previous study on multibeam IMRT combined with electrons reported V_{5Gy} doses to a 1% volume of the contralateral breast [5]. Another study reported no significant differences in contralateral breast doses for an anterior–posterior beam setting with either conformal RT or a field-in-field technique, but both methods resulted in significant contralateral doses of 12.5 Gy [11]. An objective comparison between previous results and those presented here is difficult because the PTV and OAR outlines may differ. Considering the maximum doses and V_{3Gy} volumes recorded in this work, it is however clear that the contralateral breast dose is reduced as compared with multibeam IMRT. Furthermore, it is likely that the slight increase in contralateral breast doses as compared with the standard electron/photon technique may be warranted due to a corresponding increase in PTV dose coverage. However, the PTVs medial border should anyway be considered on an individual level based on the stage of the disease and the patient's overall status.

Multifield IMRT and volumetric modified arc therapies tend to increase the mean heart dose and a value >8 Gy is not uncommon [5,6,8,18]. Five of the patients in this study had left-sided disease and independent of strategy the mean heart dose was 3.1–3.5 Gy, while mean doses for right-sided patients were 0.7–1.1 Gy (Table I). The technique presented would therefore have enabled improved medial dose coverage without unacceptable risk for cardiac-related events. Overall, our results are acceptable when compared to larger population-based studies using standard techniques that reported overall mean heart doses between 4.9 and 5.2 Gy [19,20]. Heart doses are closely related to induced risks for coronary events [20] and therefore a heart dose as low as possible should be achieved. A common, relatively new technique in left-sided breast cancer is deep inspiratory breath hold (DIBH) that increases the distance between the heart and the PTV. With a tangential beam setup the mean heart dose was reduced from 5.2 Gy to 2.7 Gy as reported in a study on 319 breast cancer patients [19]. Maintaining the OAR doses at the current level for the standard tangents, DIBH would have enabled better PTV dose coverage. However, issues regarding dose to the contralateral breast still remain.

A main drawback of the suggested method is that the beam arrangement implies a risk of gantry and couch collisions. With the equipment available at TUH patient selection was therefore limited to a chest wall height of 28 cm in the treatment position. Implementation of a 10 cm shortened electron applicator is possible [11], thereby enabling the technique in question for a larger population. However, the possible use of higher electron energies would require verification measurements due to their differing beam characteristics. Neither is it clear how the dose uniformity achieved here with 6 MeV and 9 MeV electrons would be affected by higher beam energies.

In conclusion, based on our results, the suggested method to a large extent smooths the electron and photon field junction and enables improved medial PTV dose coverage. What treatment technique is to

be preferred depends to a high degree on the patient's clinical condition, importance of treating the internal mammary nodes and finally body habitus. Standard tangential treatment is fast to treatment plan and offers good enough dose coverage for most patients, and maybe improved with DIBH. The suggested method offers better medial dose coverage within tolerable OAR doses for patients suitable for an isocentric treatment and for which the therapeutic range of 6 MeV and 9 MeV electron beams is sufficient. For the best dose coverage, a patient-wise trade-off between maximum allowed doses within the PTV and suitable OAR doses is required. At Turku University Hospital the presented method has been implemented for treatment for those patients that are suitable.

Acknowledgments

Tony Redpath is acknowledged for proof-reading.

Declaration of interest: The authors report no conflicts of interest. The authors alone are responsible for the content and writing of the paper.

References

[1] Early breast Cancer Trialists' Collaborative Group (EBCTCG). Effect of radiotherapy after mastectomy and axillary surgery on 10-year recurrence and 20-year breast cancer mortality: Meta-analysis of individual patient data for 8135 women in 22 randomised trials. Epub Lancet 2014 Mar 19.

[2] Danish Breast Cancer Cooperative Group (DBCG). DBCG Retningslinjer 5: Postoperativ strålebehandling. DBCG 2011. Available from: http://www.dbcg.dk [cited 2013 Dec 6].

[3] Pierce LJ, Butler JB, Martel MK, Normolle DP, Koelling T, Marsh RB, et al. Postmastectomy radiotherapy of the chest wall: Dosimetric comparison of common techniques. Int J Radiat Oncol Biol Phys 2002;52:1220–30.

[4] van der Laan HP, Dolsma WV, van't Veld AA, Bijl HP, Langendijk JA. Comparison of normal tissue dose with three-dimensional conformal techniques for breast cancer irradiation including the internal mammary nodes. Int J Radiat Oncol Biol Phys 2005;63:1522–30.

[5] van der Laan HP, Korevaar EW, Dolsma WV, Maduro JH, Langendijk JA. Minimising contralateral breast dose in postmastectomy intensity-modulated radiotherapy by incorporating conformal electron irradiation. Radiother Oncol 2010;94:235–40.

[6] Krueger EA, Fraass BA, McShan DL, Marsh R, Pierce LJ. Potential gains for irradiation of chest wall and regional nodes with intensity modulated radiotherapy. Int J Radiat Oncol Biol Phys 2003;56:1023–37.

[7] Beckham WA, Popescu CC, Patenaude VV, Wai ES, Olivotto IA. Is multibeam IMRT better than standard treatment for patients with left-sided breast cancer. Int J Radiat Oncol Biol Phys 2007;69:918–24.

[8] Ma J, Li J, Xie J, Chen J, Zhu C, Cai G et al. Post mastectomy linac IMRT irradiation of chest wall and regional nodes: Dosimetry data and acute toxicities. Radiat Oncol 2013;8:81.

[9] Early breast Cancer Trialists' Collaborative Group (EBCTCG). Effects of radiotherapy and of differences in the extent of surgery for early breast cancer on local recurrence and 15-year survival: An overview of the randomised trials. Lancet 2005;366:2087–16.

[10] Grantzau T, Mellemkjær L, Overgaard J. Second primary cancers after adjuvant radiotherapy in early breast cancer patients: A national population based study under the Danish Breast Cancer Cooperative Group (DBCG). Radiother Oncol 2013;106:42–9.

[11] Tenhunen M, Nyman H, Strengell S, Vaalavirta L. Linac-based isocentric electron-photon treatment of radically operated breast carcinoma with enhanced dose uniformity in the field gap area. Radiother Oncol 2009;93:80–6.

[12] Dogan N, Leybovich LB, Sethi A, Emami B. Improvement of dose distributions in abutment regions of intensity modulated radiation therapy and electron fields. Med Phys 2002;29:38–44.

[13] Recht A, Edge SB, Solin LJ, Robinson DS, Estabrook A, Fine RE, et al. Postmastectomy radiotherapy: Guidelines of the American Society of Clinical Oncology. J Clin Oncol 2001;19:1539–69.

[14] Aaltonen P, Brahme A, Lax I, Levernes S, Näslund I, Beitan JR, et al. Specification of dose delivery in radiation therapy. Recommendations by the Nordic Association of Clinical Physics (NACP). Acta Oncol 1997;36(Suppl 10):1–32.

[15] Ojala J, Hyödynmaa S, Baranczyk R, Góra E, Waligórski MPR. Performance of two commercial electron beam algorithms over regions close to lung-mediastinum interface, against Monte Carlo simulation and point dose dosimetry in virtual and anthropomorphic phantoms. Phys Med 2014;30:147–54.

[16] Abratt RP, Morgan GW. Lung toxicity following chest irradiation in patients with lung cancer. Lung Cancer 2002;35:103–9.

[17] Kwa SLS, Lebesque JV, Theuws JCM, Marks LB, Munley MT, Bentel G, et al. Radiation pneumonitis as a function of mean lung dose: An analysis of pooled data of 540 patients. Int J Radiat Oncol Biol Phys 1998;42:1–9.

[18] Nichols GP, Fontenot JD, Gibbons JP, Sanders ME. Evaluation of volumetric modulated arc therapy for postmastectomy treatment. Radiat Oncol 2014;9:66.

[19] Nissen HD, Appelt AL. Improved heart, lung and target dose with deep inspiration breath hold in a large clinical series of breast cancer patients. Radiother Oncol 2013;1,28–32.

[20] Darby SC, Ewertz M, McGale P, Bennet AM, Blom-Goldman U, Brønnum D, et al. Risk of ischemic heart disease in women after radiotherapy for breast cancer. N Engl J Med 2013;368:987–98.

Supplementary material available online

Supplementary Table I and Appendix available online at: http://informahealthcare.com/doi/abs/10.3109/0284186X.2014.926027